

Deposition of tin sulfide thin films from tin(IV) thiolate precursors

Giampaolo Barone,^{a†} Tom G. Hibbert,^a Mary F. Mahon,^a Kieran C. Molloy,^{*a} Louise S. Price,^b Ivan P. Parkin,^b Amanda M. E. Hardy^b and Mark N. Field^b

^aDepartment of Chemistry, University of Bath, Claverton Down, Bath, UK BA2 7AY.

E-mail: chskcm@bath.ac.uk

^bDepartment of Chemistry, University College, 20 Gordon Street, London, UK WC1H 0AJ

Received 20th July 2000, Accepted 20th September 2000

First published as an Advance Article on the web 16th November 2000

AACVD (aerosol-assisted chemical vapour deposition) using (PhS)₄Sn as precursor leads to the deposition of Sn₃O₄ in the absence of H₂S and tin sulfides when H₂S is used as co-reactant. At 450 °C the film deposited consists of mainly SnS₂ while at 500 °C SnS is the dominant component. The mechanism of decomposition of (PhS)₄Sn is discussed and the structure of the precursor presented.

1. Introduction

While the deposition of SnO₂ films has attracted considerable interest over a number of years,¹ routes to the formation of films of the corresponding tin sulfides are much less well studied. Several binary tin sulfides are known (SnS, SnS₂, Sn₂S₃, Sn₃S₄, Sn₄S₅)² of which only SnS, SnS₂ and Sn₂S₃ are discrete phases.³ SnS and SnS₂ are the most important, with band gaps of 1.3 and 2.18 eV, respectively.^{4,5} SnS, whose band gap lies between those of silicon (1.12 eV) and gallium arsenide (1.43 eV) has been identified for potential use in holographic recording media^{6,7} and solar control devices.^{4,8–10} The band gap for Sn₂S₃ has been reported as 0.35 eV.¹¹

Bulk materials (SnS, SnS₂) have been prepared by direct reaction of the elements,^{12–14} solid-state metathesis reactions¹⁵ and pyrolysis of organotin precursors [(R₃SnS)₃ or (R₃Sn)₂S; R = Ph, PhCH₂].^{16–18} Crystalline materials have been prepared by chemical⁵ and physical vapour transport,¹⁹ while thin films have been deposited by chemical vapour transport in ultra-high vacuum,²⁰ from solutions,^{10,21–24} by thermal evaporation²⁵ and electrochemical methods.²⁶ Spray pyrolysis of SnCl₄ and thiourea generates films of SnS₂²⁷ while the analogous use of SnCl₂ and *N,N*-dimethylthiourea can be controlled *via* the pyrolysis temperature to furnish either Sn₂S₃ or SnS.²⁸ Chemical vapour deposition (CVD) methods have the attraction of being able to coat relatively large areas at high growth rates but have received little attention. Plasma-enhanced CVD of SnCl₄/H₂S/H₂⁴ and conventional CVD of R₄Sn/H₂S/H₂ (R = Me, Et)²⁹ have been shown to deposit SnS, though the latter citation is possibly erroneous as it is based on control by the reducing atmosphere and colour rather than on film analysis. We have been interested in CVD routes to tin sulfides for potential use in solar-control and self-cleaning applications with the aim of developing an effective deposition methodology at atmospheric pressure. We have previously reported the use of SnX₄/H₂S (X = Cl,^{30,31} Br³²) as temperature-tunable dual-source atmospheric pressure CVD (APCVD) routes to SnS, Sn₂S₃ and SnS₂ and Bu₃SnO₂CCF₃/H₂S for the deposition of SnS.³³ However, single-source precursors offer an alternative methodology and one which, in principle, can negate the need for large volumes of toxic H₂S. In this paper we focus on the use of the homoleptic tin(IV) thiolate (PhS)₄Sn (**1**) as the first of

several studies to evaluate potential precursor compounds for tin sulfide deposition.

2. Experimental

Instrumentation

Infrared spectra were recorded as hexachlorobutadiene mulls between KBr plates. Measurements were made using a Nicolet 510P Fourier transform spectrometer within the range 4000–400 cm⁻¹ with a medium slit width and a peak resolution of 4.0 cm⁻¹. Carbon, hydrogen and nitrogen were determined using a Carlo-Erba Strumentazione E.A. model 1106 micro-analyser operating at 500 °C; results were calibrated against an acetanilide standard. ¹H and ¹³C NMR spectra were recorded using either Jeol JNM-GX-270FT (270 MHz) or Jeol EX-400 (400 MHz) Fourier transform spectrometers using SiMe₄ as an internal reference. ¹¹⁹Sn NMR spectra were recorded on a Jeol EX-400 (400 MHz) spectrometer; chemical shifts are relative to Me₄Sn. Details of our Mössbauer spectrometer and data handling procedures are given elsewhere.³⁴ SEM and EDAX were obtained using a Hitachi S570 Filament Scanning Electron Microscope, with a beryllium window. EDAX analyses were standardised relative to cobalt metal. EDAX data were quantified using the Oxford Instruments AM10,000 software package. Raman spectroscopy was carried out using a Dilor Infinity Raman spectrometer with a notch filter and a CCD detector coupled to an Olympus microscope. Spectra were recorded using an excitation line of wavelength 632.8 nm from a HeNe laser and calibrated against neon emission lines. X-Ray photoelectron spectra were recorded with a VG ESCALAB 220I XL instrument using monochromatic Al-K_α radiation at a pass energy of 20 eV and a spot size of 600 μm. Depth profiling was carried out using an Ar⁺ ion gun for one six minute etch. X-Ray diffraction patterns were measured on a Philips X-pert diffractometer using unfiltered Cu-K_α (λ₁ = 1.5045 Å, λ₂ = 1.5443 Å).

Synthesis

Compound **1** was synthesised by the method of Backer and Kramer.³⁵ (Phenylthiolato)sodium (9.42 g, 71.3 mmol) was added to a solution of tin tetrachloride (2.0 cm³, 17.4 mmol) in dry, degassed toluene (100 cm³) and refluxed for 2 h. After cooling to room temperature NaCl and excess sodium thiolate was removed by filtration and the resultant filtrate evaporated

†Home address: Dipartimento di Chimica Inorganica, Università di Palermo, Via Arcirafi 26–28, Palermo 90123, Italy.

to dryness *in vacuo*. Recrystallisation from diethyl ether (30 cm³) afforded **1** as colourless crystals (7.73 g, 80%). Mp 52 °C (lit. 67 °C).³⁵ Analysis, found (calculated for C₂₄H₂₀S₄Sn): C 51.4(51.9), H 3.60(3.63)%. ¹H NMR (CDCl₃): 7.20–7.58 (m, 20H, C₆H₅); ¹³C NMR (CDCl₃): 127.9, 128.7, 129.0, 135.7 (C₆H₅); ¹¹⁹Sn NMR (CDCl₃): 48.2 ppm. IR (hexachlorobutadiene mull, KBr): 3079m, 3053m, 1476s, 1438s, 743vs, 689vs cm⁻¹; Mössbauer: IS = 1.43, Γ = 0.95 mm s⁻¹.

Crystallography

A crystal of approximate dimensions 0.4 × 0.3 × 0.2 mm was used for data collection. Crystal data: C₂₄H₂₀S₄Sn, *M* = 555.33, orthorhombic, *a* = 17.192(1), *b* = 8.553(2), *c* = 8.342(1) Å, *U* = 1226.6(3) Å³, space group *Pba*2, *Z* = 2, μ(Mo-K_α) = 1.390 mm⁻¹. Crystallographic measurements were made at 293(2) K on a CAD4 automatic four-circle diffractometer in the range 2.36 < θ < 23.89°. Data (1037 reflections) were corrected for Lorentz and polarization but not for absorption. In the final least squares cycles all atoms were allowed to vibrate anisotropically. Hydrogen atoms were included at calculated positions where relevant. The solution of the structure (SHELX 86)³⁶ and refinement (SHELX 93)³⁷ converged to conventional [*i.e.* based on 729 *F*² data with *F*_o > 4σ(*F*_o)] *R*1 = 0.0527 and *wR*2 = 0.1179. Goodness of fit = 1.073. The max. and min. residual densities were 1.087 and -0.532 e Å⁻³ respectively. The asymmetric unit is shown in Fig. 1 along with the atom labelling scheme used in the text.

CCDC 1145/247. See <http://www.rsc.org/suppdata/jm/b0/b005888m/> for crystallographic files in .cif format.

Film deposition

Hydrogen sulfide (99.7%) and nitrogen (99%) gases were purchased from BOC and used as supplied. SnO₂/SiO₂-coated glass supplied by Pilkington Glass plc was used as the substrate. A Pifco Health ultrasonic humidifier Model No. 1077 was used to nebulise the precursor as solutions described elsewhere.³⁸ AACVD reactions were carried out on a horizontal-bed cold-walled reactor. Glass pre-coated with SnO₂ and a topcoating of SiO₂ was cleaned by being wiped

with petroleum spirit (bp 40–60 °C), washed with propan-2-ol and dried in air. During heating, a 0.5 dm³ min⁻¹ flow of nitrogen was passed through the system. The temperature of the glass substrate was varied between 300 and 600 °C. When the required temperature was attained, the system was left for a few minutes to reach thermal equilibrium. Tetra(phenylthiolato)stannane **1** was admitted to the system *via* the use of a nebuliser. 0.1 g of **1** was dissolved in 50 ml hexane which was poured into a modified round-bottomed flask approximately 1 cm above the piezoelectric component of the nebuliser. The flow of nitrogen through the round-bottomed flask was increased to 2 dm³ min⁻¹ and hydrogen sulfide (0.4 dm³ min⁻¹) was admitted to the system. Run times of approx. 20 min were marked by the turning on and off of the humidifier at the start and end of the experiment. After the reaction, the hydrogen sulfide flow was stopped. The heater was turned off and the glass and reactor allowed to cool to room temperature under a 0.5 dm³ min⁻¹ flow of nitrogen.

3. Results and discussion

Synthesis and crystallography

Compound **1** was synthesised by the reaction of NaSPh and SnCl₄ in toluene (80% yield) following established procedures.^{35,39,40} The compound is air stable with a pungent odour. Crystals suitable for crystallography were obtained from ether.

The structure of **1** is shown in Fig. 1 and, to our knowledge, is the only simple homoleptic tin(IV) thiolate structurally characterised to date, though those of the functionalised species (PyS)₄Sn⁴¹ and [MeS(Ph)C=C(Ph)S]₄Sn⁴² have been reported. The asymmetric unit of **1** consists of one half of a molecule with the central tin atom seated on a 2-fold rotation axis implicit in the space group symmetry. The remaining portion of the molecule is generated *via* the symmetry operation 1 - *x*, -*y*, *z*. The coordination about tin is, perhaps not surprisingly, tetrahedral, in contrast to the corresponding (RO)₄Sn species which, having higher Lewis acidity due to the more polar Sn–O bonds, expand their coordination spheres by dimerisation (μ-OR bridged) and/or solvation by ROH.^{43,44} The structure of [MeS(Ph)C=C(Ph)S]₄Sn, which incorporates a ligand predisposed to chelation, does however show two sets of Sn–S bonds corresponding to the strong covalent [2.436(1) Å] and weaker coordinate [3.599(2) Å] Sn–S interactions.⁴²

The Sn–S bonds in **1** [2.379(4), 2.401(4) Å] are consistent with, but generally shorter than, those in related species such as Ph₃SnSPh [2.421(1) Å], Ph₂Sn(SPh)₂ [2.410(2) Å],⁴⁵ Ph₃Sn(SC₁₀H₇) [2.418(1) Å], Me₂Sn(SC₁₀H₇)₂ [2.418(4), 2.411(3) Å]⁴⁶ and [MeS(Ph)C=C(Ph)S]₄Sn. The S–Sn–S bond angles about tin [114.9(2), 107.8(1), 106.0(1)°] show deviations from the ideal which, although small, are unexpected in a perfectly symmetrical molecule free from internal congestion. While such features are conveniently dismissed as arising from packing effects such an analysis clouds what appears to be a subtle bonding feature. Almost identical angular distortions are observed in the primary (tetrahedral) coordination sphere of [MeS(Ph)C=C(Ph)S]₄Sn [107.0(1), 114.5(1)°] and we have noted S–Sn–S angles in the range 99.2–117.2° amongst the related species (CyS)₄Sn and (tBuS)₄Sn.⁴⁷ E–M–E angular distortions in the range 100.4–117.4° have been reported for other members of the generic series (RE)₄M (M = C, Si, Ge, Sn; E = O, S, Se). These angular variations can be modelled by AM1 calculations on isolated molecules,⁴⁷ again mitigating against packing effects, and appear to be associated with bonding MOs involving E···E interactions along with the conformational preferences for the various C–S–Sn–S units. We will report more fully on this matter elsewhere.

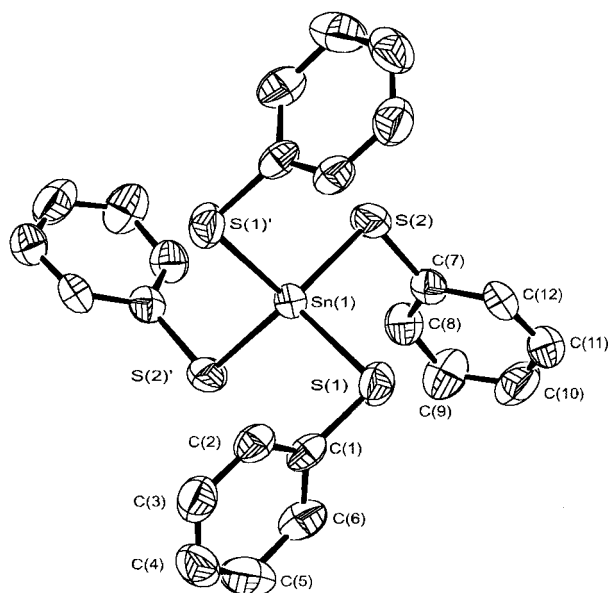


Fig. 1 ORTEX⁶³ plot of the asymmetric unit of **1**. Thermal ellipsoids are at the 30% probability level. Selected metric data: Sn(1)–S(1) 2.379(4), Sn(1)–S(2) 2.401(4), S(1)–C(1) 1.76(1), S(2)–C(7) 1.78(1) Å; S(1)–Sn(1)–S(1') 114.9(2), S(1)–Sn(1)–S(2) 106.0(1), S(1')–Sn(1)–S(2) 107.8(1), C(1)–S(1)–Sn(1) 98.2(4), C(7)–S(2)–Sn(1) 98.5(4)°.

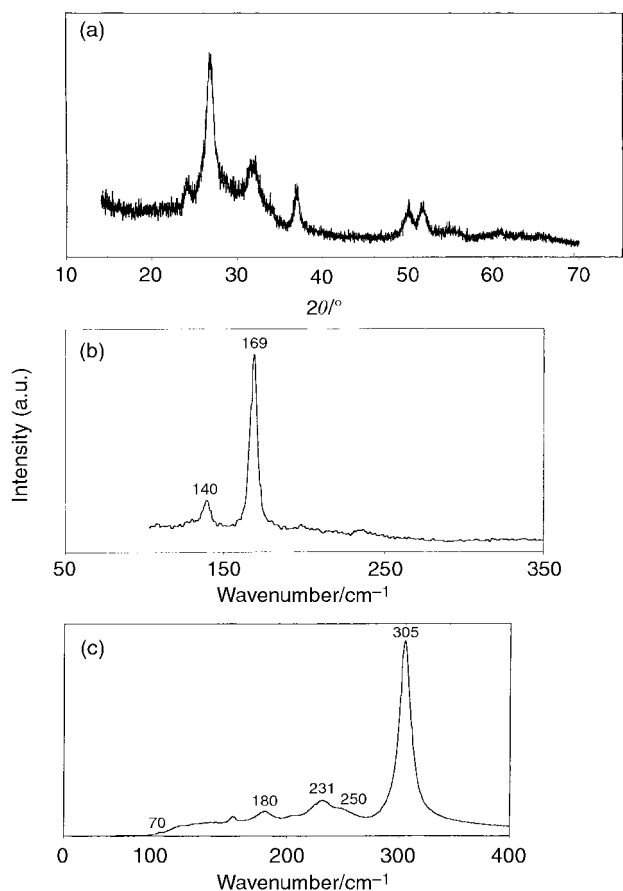


Fig. 2 XRD pattern (a) and Raman spectrum (b) for the film produced from the CVD of **1** in the absence of H_2S , identified as Sn_3O_4 . The Raman spectrum of the film after heating at $500\text{ }^\circ\text{C}$ in a stream of H_2S , identified as Sn_2S_3 , is also shown (c).

Decomposition and deposition studies

In the absence of H_2S (*i.e.* using 99.9% N_2) the films produced do not contain sulfur. The XRD pattern (Fig. 2a) is identical to that previously reported for Sn_3O_4 (PDF 16-0737) and shows no peaks assignable to SnO_2 or SnO . The broad peaks are indicative of nanocrystalline material but it is difficult to get accurate crystal sizes in such materials because of preferred orientation effects. Further confirmation of the film composition comes from the Raman spectrum (Fig. 2b) which shows two bands ($140, 169\text{ cm}^{-1}$) that compare well with literature data for Sn_3O_4 ($145, 171\text{ cm}^{-1}$).^{48,49} Sn_3O_4 was first reported in 1967⁵⁰ and subsequently identified as being formed either when SnO disproportionates in the range $250\text{--}450\text{ }^\circ\text{C}$ ⁵¹ or is partially oxidised.⁴⁸

The preferential deposition of oxide, rather than sulfide, films even when only traces of oxygen are present in the carrier gas has been noted by others. For example, decomposition of $\text{Bu}_2\text{InSPr}^1$ under CVD conditions yields In_2S_3 only when 99.999% Ar is the carrier gas. When 99.99% or lower purity Ar is used In_2O_3 is formed and the rate of oxide formation is faster for Ar containing 0.1% O_2 than when 1% O_2 is present. The authors postulate that a sulfide film (InS , In_2S_3) is the primary deposition product but that it is readily oxidised by small amounts of O_2 in the carrier gas.⁵² However, we see no evidence for oxide formation when the sulfide is deposited under a partial pressure of H_2S followed by cooling the film in N_2 alone, which suggests that in the absence of H_2S it is the oxide which is formed directly.

While bulk and vapour phase decompositions can follow different routes, the former can afford useful clues as to the nature of the CVD process. Thus, we have carried out the thermal decomposition of bulk **1** and examined the products as a function of temperature by Mössbauer spectroscopy. After 2 h heating at $200\text{ }^\circ\text{C}$ in a dried Schlenk tube under dynamic vacuum, all traces of **1** (Fig. 3a) are gone and the spectrum consists of a high velocity doublet ($\text{IS}=3.00$, $\text{QS}=1.99$, $\Gamma=1.23\text{ mm s}^{-1}$, 66%) and a narrow doublet typical of SnO_2 ($\text{IS}=0.12$, $\text{QS}=0.58$, $\Gamma=1.10\text{ mm s}^{-1}$, 34%) (Fig. 3b). The major component is clearly Sn(II) and has parameters similar to those recorded for $(\text{PhS})_2\text{Sn}$ ($\text{IS}=3.19$, $\text{QS}=1.70$, $\Gamma=1.10\text{ mm s}^{-1}$) which was prepared by a literature route. After a further 2 h at $300\text{ }^\circ\text{C}$, the Sn(II) component has largely disappeared and the spectrum is dominated by SnO_2 (Fig. 3c). The clear inference is that **1** decomposes initially by loss of PhSSPh to yield $(\text{PhS})_2\text{Sn}$, and this process is aided by the close $\text{S}\cdots\text{S}$ contacts (narrow $\langle\text{S}\text{--}\text{Sn}\text{--}\text{S}\rangle$ seen in the structure of **1** (Fig. 1). The genesis of SnO_2 could either be by oxidative decomposition of the Sn(II) species directly, or by further elimination of PhSSPh to leave highly reactive Sn(0) . While we have no direct evidence for the *in situ* formation of tin metal, the ease of formation of tin oxides (both here and in the CVD process) is consistent with a highly reactive intermediate. Others have reported that decomposition of $(\text{BuS})_2\text{Pb}$ (various isomers) yields PbS contaminated by traces of Pb and PbO , the oxide being ascribed to post synthesis oxidation of the metal.⁵³ In addition, the EI mass spectrum (70 eV) of **1** remarkably involves no tin-containing fragments. The two fragments which dominate the spectrum occur at m/z of 109 and 218, corresponding to PhS and PhSSPh , respectively. Furthermore, we have observed in other aspects of this study that $(\text{C}_6\text{H}_{11}\text{S})_2\text{Sn}$, when heated to *ca.* $100\text{ }^\circ\text{C}$ deposits a tin mirror on the walls of the reaction vessel and that Sn_3O_4 has recently been identified as the product of the thermal oxidation of tin metal on glass at *ca.* $450\text{ }^\circ\text{C}$.⁴⁸ In the TGA of **1**, weight loss begins at $186\text{ }^\circ\text{C}$ and continues gradually up to $390\text{ }^\circ\text{C}$. The

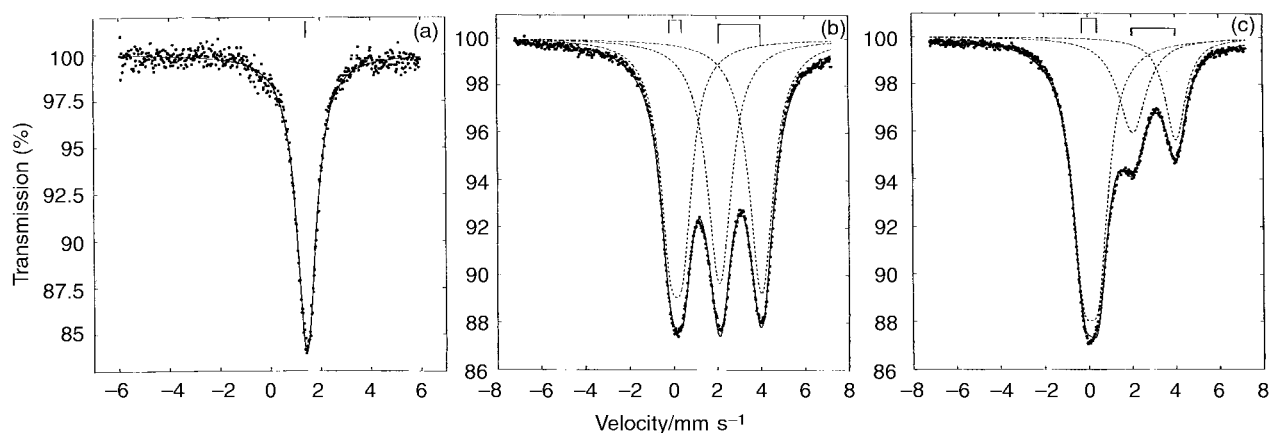


Fig. 3 Mössbauer spectra of (a) **1**, (b) **1** heated for 2 h at $200\text{ }^\circ\text{C}$ and (c) further heating for 2 h at $300\text{ }^\circ\text{C}$, both under dynamic vacuum.

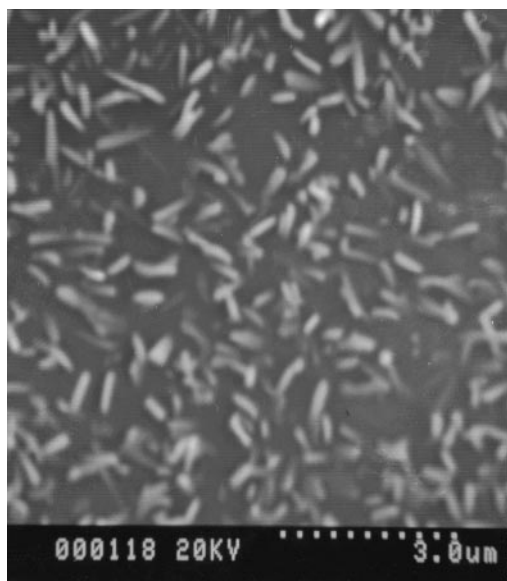


Fig. 4 SEM of the film produced by the decomposition of **1** in a flow of H_2S ($0.4 \text{ dm}^3 \text{ min}^{-1}$) at 500°C .

residue corresponds to 25.3% of the original mass which correlates well with the composition being Sn_3O_4 (*i.e.* $\text{SnO}_{1.33}$ corresponds to a theoretical 25.2% residual weight).

Other reports on the decomposition of $(\text{RS})_2\text{M}$ reveal that elimination of R_2S is most commonly observed, with MS as residue.^{53–55} Both Bu_2S (*i*-, *s*-Bu isomers) and BuSSBu (*t*-Bu isomers) have been identified as by-products in the decomposition of $(\text{BuS})_2\text{Pb}$ (*t*-, *s*-, *i*-Bu isomers), though the disulfide can be explained as arising from decomposition of $^i\text{Bu}_2\text{S}$.⁵³ On the other hand, $\text{Hg}(\text{TeR})_2$ decomposes to Hg and RTeTeR ⁵⁶ and it is known that $(\text{RS})_4\text{Sn}$ can be prepared by oxidative addition of RSSR to tin metal.⁵⁷

With *ca.* 10% H_2S added to the carrier gas tin sulfide films were produced which were either yellow in colour (deposited at 450°C) or grey for deposition at higher temperatures (500 and 550°C). SnS_2 is yellow with a metallic lustre⁵ and SnS is grey/black in colour.¹³ By Scanning Electron Microscopy (SEM) the films appeared to be composed of small particles approximately $1 \mu\text{m}$ long and 100 nm wide. There were large areas of glass visible between the particles (Fig. 4). The films were not particularly adherent to the glass, and while they passed the Scotch tape test they could be removed from the substrate with a scalpel.

Both tin and sulfur were observed in the films by Energy Dispersive Analysis by X-rays (EDAX). It was impossible to determine the precise composition of the films by this technique as most of the excitation volume studied was comprised of the underlying glass due to the thin coverage of the substrate by the film. By X-ray photoelectron spectroscopy the tin $3d_{5/2}$ binding energy was found to be 485.6 eV for the film deposited at 500°C which corresponds to SnS , and 485.9 eV for the film deposited at 450°C which is indicative of tin in a higher oxidation state (*i.e.* SnS_2).⁵⁸ For the film deposited at 500°C a shoulder was seen on the surface at 486.6 eV which is the binding energy of SnO_2 ⁵⁹ and this is most likely due to surface oxidation since this shoulder disappeared after etching. The sulfur $2p$ binding energy was observed to be 153.5 eV .

Raman microscopy showed that the films were not phase pure. The film deposited at 450°C was found to be predominantly SnS_2 with some SnS (Fig. 5a) and the film deposited at 500°C was found to be predominantly SnS with traces of SnS_2 (Fig. 5b). It has previously been reported that the Raman spectrum of the 2H-polytype of tin(IV) sulfide has its principal band at 317 cm^{-1} with a weaker band at 209 cm^{-1} ⁶⁰ due to the intra-layer modes of A_g and E symmetry,

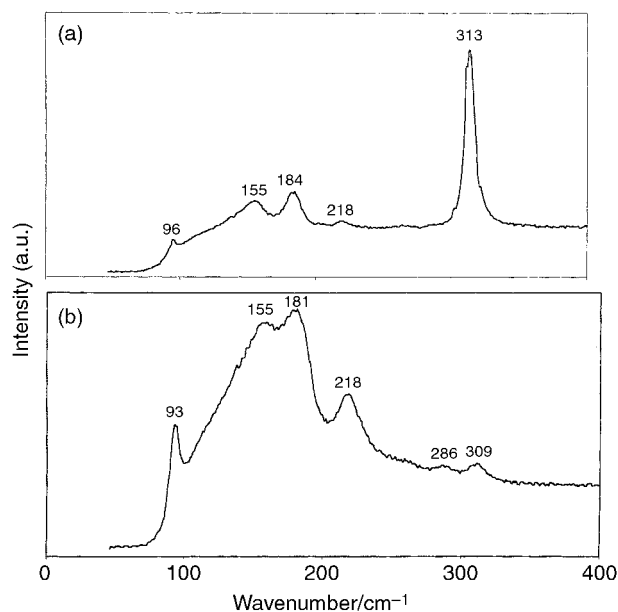


Fig. 5 Raman spectra of films produced by the CVD of **1** at 450°C (a) SnS_2 with traces of SnS and 500°C , (b) SnS with traces of SnS_2 , both with a flow of $0.4 \text{ dm}^3 \text{ min}^{-1}$ H_2S .

respectively. The spectrum of tin(II) sulfide, as reported previously,⁶¹ has Raman bands at 218, 189, 160 and 94 cm^{-1} corresponding to crystallites of tin(II) sulfide with random orientations. The films were too thin to be analysed by reflectance X-ray diffraction.

SnS_2 films are stable up to 400°C but at 550°C convert to primarily SnS , as evidenced by a Raman spectrum qualitatively identical to that of Fig. 5b, save for a greater intensity to the band at 218 cm^{-1} . A stream of H_2S ($0.4 \text{ dm}^3 \text{ min}^{-1}$) facilitates the reduction, such that under these conditions SnS_2 is partially reduced to Sn_2S_3 at 500°C (the Raman spectrum closely resembles that of Fig. 2c) while at higher temperatures complete reduction to SnS is achieved (Raman data: 217, 189, 159, 95 cm^{-1}). These observations have clear implications for the temperature-controlled CVD of tin sulfides in the presence of H_2S .

It is important to note the previous CVD routes for the deposition of tin sulfide films either use H_2S as co-reactant^{4,29–32} or use reagents which are likely to generate H_2S *in situ* during decomposition *e.g.* thiourea.^{27,28} Spray pyrolysis of $\text{SnCl}_2/N,N$ -dimethylthiourea also leads to SnO_2 films at $T=450^\circ\text{C}$, although sulfide films are deposited at lower temperatures.²⁸ Moreover, we have found that Sn_3O_4 films produced in the absence of H_2S can be converted to tin sulfide films on heating in a stream of the latter gas. The Raman spectrum of the resulting material (Fig. 2c) shows peaks at 305, 250, 231, 180 and 70 cm^{-1} which are all present in the reference spectrum of Sn_2S_3 .⁶² The formation of a mixed-valence tin sulfide from a mixed-valence tin oxide (Sn_3O_4) is perhaps not surprising.

4. Conclusions

Tin(IV) thiolates, typified by $(\text{PhS})_4\text{Sn}$, can be used for the deposition of tin sulfide films by aerosol-assisted CVD, provided the carrier gas contains *ca.* 10% H_2S . The films produced are dependent on the deposition temperature, with predominantly SnS_2 produced at $T < 500^\circ\text{C}$ and SnS at $T > 500^\circ\text{C}$. The temperature regimes are insufficiently distinct to lead to phase-pure films. In the absence of H_2S only Sn_3O_4 films are observed, highlighting the preferential formation of oxide films in the absence of a secondary sulfur source.

Acknowledgements

We thank the EPSRC and Pilkington Glass plc for financial support and Professor R. J. H. Clark for helpful discussions.

References

- 1 K. L. Chopra, S. Major and D. K. Pandya, *Thin Solid Films*, 1983, **102**, 1.
- 2 T. Jiang and G. A. Ozin, *J. Mater. Chem.*, 1998, **8**, 1099.
- 3 R. C. Sharma and Y. A. Chang, *Bull. Alloy Phase Diagrams*, 1986, **7**, 269.
- 4 A. Ortiz, J. C. Alonso, M. Garcia and J. Toriz, *J. Semicond. Sci. Technol.*, 1996, **11**, 243.
- 5 S. K. Arora, D. H. Patel and M. K. Agarwal, *J. Mater. Sci.*, 1994, **29**, 3979.
- 6 G. Valiukonis, D. A. Guseinova, G. Krivaite and A. Sileica, *Phys. Status Solidi B*, 1990, **135**, 299.
- 7 M. Radot, *Phys. Appl.*, 1977, **18**, 345.
- 8 J. P. Singh and R. K. Bedi, *Thin Solid Films*, 1991, **199**, 9.
- 9 P. K. Nair, M. T. S. Nair, A. Fernandez and M. Ocampo, *J. Phys. D: Appl. Phys.*, 1989, **22**, 829.
- 10 M. T. S. Nair and P. K. Nair, *Semicond. Sci. Technol.*, 1991, **6**, 132.
- 11 U. V. Alpen, J. Fenner and E. Gmelin, *Mater. Res. Bull.*, 1975, **10**, 495.
- 12 H. Martinez, C. Auriel, M. Loudet and G. Pfister-Guillouzo, *Appl. Surf. Sci.*, 1996, **103**, 149.
- 13 G. A. Shaw and I. P. Parkin, *Main Group Met. Chem.*, 1996, **19**, 499.
- 14 R. Coustal, *J. Chim. Phys.*, 1931, **31**, 277.
- 15 I. P. Parkin and A. T. Rowley, *Polyhedron*, 1993, **12**, 2961.
- 16 S. R. Bahr, P. Boudjouk and G. J. McCarthey, *Chem. Mater.*, 1992, **4**, 383.
- 17 P. Boudjouk, D. J. Seidler, S. R. Bahr and G. J. McCarthey, *Chem. Mater.*, 1994, **6**, 2108.
- 18 P. Boudjouk, D. J. Seidler, D. Grier and G. J. McCarthey, *Chem. Mater.*, 1996, **8**, 1189.
- 19 S. K. Arora, D. H. Patel and M. K. Agarwal, *J. Cryst. Growth*, 1993, **131**, 268.
- 20 R. Schlaf, N. R. Armstrong, B. A. Parkinson, C. Pettenkofer and W. Jaegermann, *Surf. Sci.*, 1997, **385**, 1.
- 21 M. Ristov, G. Sinadinovski, I. Grozdanov and M. Mitreski, *Thin Solid Films*, 1989, **173**, 53.
- 22 R. Engelken, H. McCloud, M. Slayton and E. Smith, *J. Electrochem. Soc.*, 1975, 134.
- 23 C. D. Lokhande, *J. Phys. D: Appl. Phys.*, 1990, **23**, 1703.
- 24 S. Kunnoudi, T. Nakazawa, A. Ashida and N. Yamamoto, *Sol. Energy Mater. Sol. Cells*, 1994, **35**, 185.
- 25 K. Deraman, S. Sakrani, B. Bismail, Y. Wahab and R. D. Gould, *Int. J. Electron.*, 1994, **76**, 917.
- 26 S. A. Jodgudri, U. K. Mohite, K. M. Gadave and C. D. Lokhande, *Ind. J. Pure Appl. Phys.*, 1994, **32**, 772.
- 27 A. K. Abass, K. M. Majeid and W. A. Murad, *Solid State Commun.*, 1986, **57**, 805.
- 28 S. Lopez and A. Ortiz, *Semicond. Sci. Technol.*, 1994, **9**, 2130.
- 29 H. M. Manasevit and W. I. Simpson, *J. Electrochem. Soc.*, 1975, **122**, 444.
- 30 L. S. Price, I. P. Parkin, T. G. Hibbert and K. C. Molloy, *Adv. Mater.*, 1998, **4**, 222.
- 31 L. S. Price, I. P. Parkin, A. M. E. Hardy, R. J. H. Clark, T. G. Hibbert and K. C. Molloy, *Chem. Mater.*, 1999, **11**, 1792.
- 32 I. P. Parkin, L. S. Price, A. M. E. Hardy, R. J. H. Clark, T. G. Hibbert and K. C. Molloy, *J. Phys. IV*, 1999, **9**, 8.
- 33 L. S. Price, I. P. Parkin, M. N. Field, A. M. E. Hardy, R. J. H. Clark, T. G. Hibbert and K. C. Molloy, *J. Mater. Chem.*, 2000, **10**, 527.
- 34 K. C. Molloy, T. G. Purcell, K. Quill and I. Nowell, *J. Organomet. Chem.*, 1984, **267**, 237.
- 35 H. J. Backer and J. Kramer, *Recl. Trav. Chim. Pays-Bas*, 1934, **53**, 1101.
- 36 G. M. Sheldrick, SHELX 86, A Computer Program for Crystal Structure Determination, University of Göttingen, Göttingen, 1986.
- 37 G. M. Sheldrick, in SHELX 93, A Computer Program for Crystal Structure Refinement, University of Göttingen, Göttingen, 1993.
- 38 D. A. Edwards, R. M. Harker, M. F. Mahon and K. C. Molloy, *J. Mater. Chem.*, 1999, **9**, 1771.
- 39 R. C. Poller and J. N. R. Ruddick, *J. Chem. Soc., Dalton Trans.*, 1974, 146.
- 40 J. D. Kennedy, W. McFarlane, G. S. Payne, P. L. Clarke and J. L. Wardell, *J. Chem. Soc., Perkin Trans. 2*, 1975, 1234.
- 41 L. C. Damude, P. A. W. Dean, V. Manivannan, R. S. Srivastava and J. J. Vittal, *Can. J. Chem.*, 1990, **68**, 1323.
- 42 G. N. Schrauzer, R. K. Chadha, C. Zhang and H. K. Reddy, *Chem. Ber.*, 1993, **126**, 2367.
- 43 M. J. Hampden-Smith, T. A. Wark, A. L. Rheingold and J. C. Huffman, *Can. J. Chem.*, 1990, **69**, 121.
- 44 C. D. Chandler, J. Caruso, M. J. Hampden-Smith and A. L. Rheingold, *Polyhedron*, 1995, **14**, 2491.
- 45 N. L. Speziali, B. G. Guimares, R. M. Silva, P. H. Duarte and S. R. Aguiar, *Acta Crystallogr., Sect. C*, 1994, **50**, 1059.
- 46 A. Kalsoom, M. Mazhar, S. Ali, M. F. Mahon, K. C. Molloy and M. I. Chaudry, *Appl. Organomet. Chem.*, 1997, **11**, 47.
- 47 T. G. Hibbert, M. F. Mahon, K. C. Molloy, I. P. Parkin, L. S. Price and I. Silaghi-Dumitrescu, unpublished work.
- 48 L. Sangaletti, L. E. Depero, B. Allieri, F. Pioselli, E. Comini, G. Sberveglieri and M. Zocchi, *J. Mater. Res.*, 1998, **13**, 2457.
- 49 J. Geurts, S. Rao, W. Richter and F. J. Schmitte, *Thin Solid Films*, 1984, **121**, 217.
- 50 F. Lawson, *Nature*, 1967, **215**, 955.
- 51 F. Gauzzi, B. Verdini, A. Maddalena and G. Principi, *Inorg. Chim. Acta*, 1985, **104**, 1.
- 52 R. Nomura, K. Konishi and H. Matsuda, *J. Electrochem. Soc.*, 1991, **138**, 631.
- 53 G. Kräuter, P. Favreau and W. S. Rees, *Chem. Mater.*, 1994, **6**, 543.
- 54 T. Yamamoto and Y. Sekine, *Inorg. Chim. Acta*, 1984, **83**, 47.
- 55 K. Osakada and T. Yamamoto, *Inorg. Chem.*, 1991, **30**, 2328.
- 56 M. L. Steigerwald and C. R. Sprinkle, *J. Am. Chem. Soc.*, 1987, **109**, 7200.
- 57 R. Kumar, H. E. Mabrouk and D. G. Tuck, *J. Chem. Soc., Dalton Trans.*, 1988, 1045.
- 58 C. D. Wagner, *Discuss. Faraday Soc.*, 1975, **60**, 291.
- 59 A. W. C. Lin, N. R. Armstrong and T. Kuwana, *Anal. Chem.*, 1997, **49**, 1228.
- 60 H. Katahama, S. Nakashima, A. Mitsuishi, M. Ishigame and H. Arashi, *J. Phys. Chem. Solids*, 1983, **44**, 1081.
- 61 H. R. Chandrasekhar, R. G. Humphries, U. Zwick and M. Cordona, *Phys. Rev. B*, 1977, **15**, 2177.
- 62 H. R. Chandrasekhar and D. G. Mead, *Phys. Rev.*, 1979, **19**, 932.
- 63 P. McArdle, *J. Appl. Crystallogr.*, 1995, **28**, 65.